

Surface representations for 3D face recognition

Thomas Fabry*, Dirk Smeets* and Dirk Vandermeulen
Katholieke Universiteit Leuven
Belgium

1. Introduction

For long, face recognition has been a 2D discipline. However, 2D face recognition has shown to be extremely difficult to be robust against a.o. lighting conditions and pose variations (Phillips et al., 2003). At the same time, technological improvements are making 3D surface capturing devices affordable for security purposes. As a result of these recent developments face recognition shifts from 2D to 3D. This means that in the current state-of-the-art face recognition systems the problem is no longer the comparison of 2D color photos, but the comparison of (textured) 3D surface shapes.

With the advent of the third dimension in face recognition, we think it is necessary to investigate the known surface representations from this point of view. Throughout recent decades, a lot of research focused on finding an appropriate digital representation for three dimensional real-world objects, mostly for use in computer graphics (Hubeli & Gross, 2000; Sigg, 2006). However, the needs for a surface representation in computer graphics, where the primary concerns are visualization and the ability to process it on dedicated computer graphics hardware (GPUs), are quite different from the needs of a surface representation for face recognition.

Another motivation for this work is the non-existence of an overview of 3D surface representations, although the problem of object representation is studied since the birth of computer vision (Marr, 1982).

With this in mind, we will, in this chapter, try to give an overview of surface representations for use in biometric face recognition. Also surface representations that are not yet reported in current face recognition literature, but we consider to be promising for future research – based on publications in related fields such as 3D object retrieval, computer vision, computer graphics and 3D medical imaging – will be discussed.

What are the desiderata for a surface representation in 3D face recognition? It is certainly useful for a surface representation in biometric applications, to be accurate, usable for all sorts of 3D surfaces in face recognition (open, closed...), concise (efficient in memory usage), easy to acquire/construct, intuitive to work with, have a good formulation, be suitable for computations, convertible in other surface representations, ready to be efficiently displayed and useful for statistical modelling. It is nevertheless also certainly necessary to look further than a list of desiderata. Therefore, our approach will be the following: we make a taxonomy of all surface representations within the scope of 3D face recognition. For each of the of the representations in this taxonomy, we will shortly describe the mathematical theory behind it. Advantages and disadvantages of the surface representation will be stated. Related research using these representations will be discussed and directions for future research will be indicated.

*The first two authors have equal contribution in this work .

The structure of this chapter follows the taxonomy of Fig. 1. First we discuss the explicit (meshfree) surfaces in section 2, followed by the implicit surfaces in section 3. We end with some conclusions regarding surface representations for 3D face recognition.

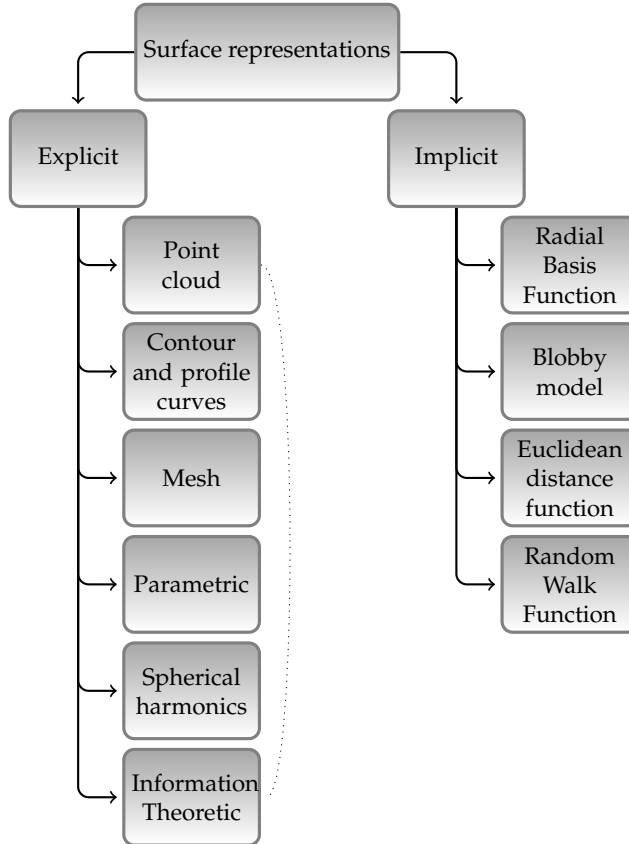


Fig. 1. Overview of surface representations

2. Explicit surface representations

In this section, several explicit surface representations are discussed. Strictly speaking, explicit functions $f(\vec{x}) : \mathbb{R}^m \rightarrow \mathbb{R}^n$ are functions in which the n dependent variables can be written explicitly in terms of the m independent variables. Simple shapes (spheres, ellipsoids,...) can be described by analytic functions. Unfortunately, it is mostly not possible to represent real world objects by analytical surfaces. Therefore, this section mainly focusses on discretised surface representations.

2.1 Point clouds

The point cloud is without doubt the simplest surface representation. It consists of an unordered set of points that lie on the surface, in the 3D case an unordered set of x , y , and

z -coordinates. While a point cloud is not a real surface representation, but a (sometimes very) sparse approximation of the surface at certain well-defined points, we consider this representation for a number of reasons. Firstly, point clouds are most often the output created by 3D scanners. Secondly, the point cloud can be the base of most of the following surface representations. Another reason to incorporate the point cloud in this document is its increased popularity because of the ever-increasing memory capacities in today's computers. Earlier the amount of stored information was to be minimized, so a minimal amount of points were stored. As these point clouds were very sparse and as such a very coarse approximation of the surface, they were then interpolated using, for instance, tensor-product splines. Today, memory shortage is of less concern, so more points can be stored, making point clouds approximate other surface representations on finer and finer levels of detail.

Figure 2 gives an example of a 3D face represented as a point cloud, containing approximately 2000 points.

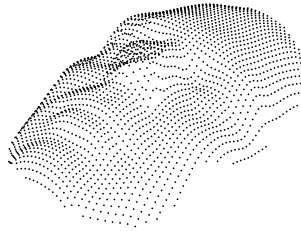


Fig. 2. An example of a 3D face represented as a point cloud.

One big advantage of the point cloud surface representation is the easy editing of point clouds: because of the lack of a global connectivity graph or parameterization, point insertion, deletion, repositioning, ... is trivial. Another important advantage is the large amount of algorithms developed for point clouds. A very popular method for 3D surface alignment, the Iterative Closest Point (ICP) algorithm (Besl & McKay, 1992), uses only points on both surfaces and iterates between closest points search for correspondence finding and transformation calculation and application. Afterwards, many variants of the original algorithm were developed (Rusinkiewicz & Levoy, 2001). The main drawback of point clouds is the incompleteness of the surface description: only at some sparse point locations the surface is known. Therefore, by representing a surface by a point cloud, a trade-off has to be made between accuracy and amount of stored information. Also, rendering a set of points as a smooth surface needs special processing, as explained in (Fabio, 2003).

The earliest use of point clouds was as a rendering primitive in (Levoy & Whitted, 1985). Point clouds have also been used for shape and appearance modeling in e.g. (Kalaiah & Varshney, 2003; Pauly et al., 2003).

In 3D face recognition, point clouds are frequently used. Mostly for surface registration with ICP (Alyüz et al., 2008; Amberg et al., 2008; Chang et al., 2006; Faltemier et al., 2008; Kakadiaris et al., 2007; Lu & Jain, 2006; Maurer et al., 2005; Russ et al., 2006; Wang et al., 2006). Bronstein et al. (2005) represent faces by an expression-invariant canonical form, i.e. a point cloud where

point wise Euclidean distances approximately equal the point wise geodesic distances¹ in the original face representation. Three-dimensional face shapes are often modeled with a point cloud based statistical model, mostly a PCA model as in (Al-Osaimi et al., 2009; Amberg et al., 2008; Lu & Jain, 2006; Russ et al., 2006). In Mpiperis et al. (2008), a bilinear model, based on point clouds, is used to separate intra-class and inter-class variations. In Fabry et al. (2008), point clouds are treated in an information theoretic way, leading to probability density function as surface representation, which is discussed in more detail in section 2.6.

2.2 Contour and profile curves

Contour and profile curves are also very sparse surface representations. They can even be sparser than point clouds, but can also be made to approximate the surface as good as wanted. The main idea is to represent shapes by the union of curves. The curves itself can be represented by a set of connected points or as a parametric curve.

Contour curves are closed, non intersecting curves on the surface, mostly of different length. Depending on the extraction criterion, different types of contour curves can be defined. Iso-depth curves are obtained by translating a plane through the 3D face in one direction and considering n different intersections of the plane and the object. n is the number of contours that form the surface representation. Mostly the plane is positioned perpendicular to and translated along the gaze direction, which is hereby defined as the z -axis. Then iso-depth curves have equal z -values. Iso-radius curves are contours, obtained as an intersection of the object with a cylinder with radius $r = \sqrt{x^2 + y^2}$, or as an intersection with a sphere with radius $r = \sqrt{x^2 + y^2 + z^2}$, with the z -axis parallel to the gaze direction and the y -axis parallel to the longitudinal axis of the face. An iso-geodesic curve, or iso-geodesic, is a contour with each part of the curve on an equal geodesic distance to a reference point, i.e. the distance of the shortest path on the full surface between the part of the curve and the reference point. The calculation of geodesic distances is mostly done using a polygon mesh (see section 2.3).

Examples of iso-depth, iso-radius and iso-geodesic curves are given in Fig. 3. Only points lying on those curves are shown.

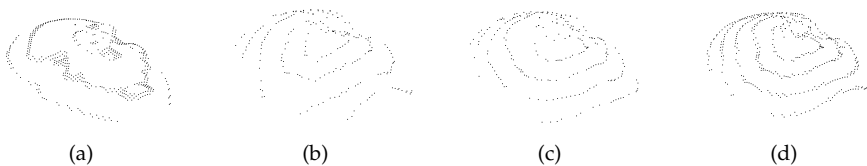


Fig. 3. Points lying on iso-depth curves (a), on iso-radius curves obtained by intersection with a cylinder (b) or with a sphere (c) and iso-geodesics with respect to the nose tip (d).

Profile curves on the contrary have a starting and an end point. For 3D faces, the starting point is most frequently a point in the middle of the face, mostly the nose tip, while the end point is often at the edge of the face. There exist an infinite number of profile curves in between those points. Figure 4(a) shows an example with each part on the curve having the same angle with respect to a line in the xy -plane through the central point (nose tip). Figure 4(b) shows points

¹ The geodesic distance is the length of the shortest path on the object surface between two points on the object.

on lines with equal x -value, again with the z -axis parallel to the gaze direction and the y -axis parallel to the longitudinal axis.

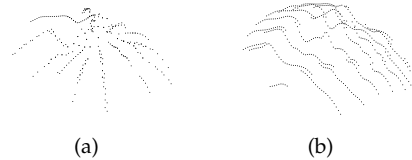


Fig. 4. Points on profile curves with curve parts under the same angle (a) or with the same x -value (b).

Curves are non-complete surface representations, implying that the surface is only defined on the curves. On the one hand, this implies a loss of information, on the other hand lower storage requirements. In order to construct contour curves, a reference point is needed. In 3D face recognition mostly the nose is used, which infers the manual or automatic extraction of this landmark. For extraction of iso-depth and cylinder based iso-radius curves and most types of profile curves, even more information is required: the gaze direction and/or longitudinal axis of the face. When done this, it is more easy to set correspondences between faces based on corresponding curves.

Contour and profile curves are frequently used in 3D face recognition. Iso-geodesics are popular because of their lower sensitivity to expression variation, based on the hypothesis that expression-induced surface variations can approximately be modeled by isometric transformations. Those transformations keep geodesic distances between every point pair on the surface. Berretti et al. (2006) use the spatial relationship between the intra-subject iso-geodesics as a subject specific shape descriptor. Feng et al. (2007) divide the iso-geodesics in segments that form the basis of trained face signatures. Mpiperis et al. (2007) map the iso-geodesic curves to concentric circles on a plane using a piecewise linear warping transformation. Jahanbin et al. (2008) extract five shape descriptors from each iso-geodesic: convexity, ratio of principal axes, compactness, circular and elliptic variance. These features are trained with Linear Discriminant Analysis (LDA). In Li et al. (2008), LDA is also used for training of texture intensities sampled at fixed angles on iso-geodesic curves. Pears & Heseltine (2006) use sphere based iso-radius curves. Due to the infinite rotational symmetry of a sphere, the representation is invariant to pose variations. Using this representation, registration can be implemented using a simple process of 1D correlation resulting in a registration of a comparable accuracy to ICP, but fast, non iterative, and robust to the presence of outliers. Samir et al. (2006) compare faces using dissimilarity measures extracted from the distances between iso-depth curves. Jahanbin et al. (2008) use iso-depth curves in the same way as they use iso-geodesics. Profile curves are used by ter Haar & Veltkamp (2008), where comparison is done using the weighted distance between corresponding sample points on the curves, and in Feng et al. (2006) where the curves are used similar as in Feng et al. (2007) (see above).

2.3 Polygon meshes

In 3D research in general, and a fortiori in 3D face recognition, the vast majority of researchers represent 3D object surfaces as meshes. A mesh is in essence an unordered set of vertices (points), edges (connection between two vertices) and faces (closed set of edges) that together

represent the surface explicitly. Mostly, the faces consist of triangles, quadrilaterals or other simple convex polygons, since this simplifies rendering. Figure 5 shows the triangular mesh corresponding with the point cloud of Fig. 2.

The problem of constructing a mesh given a point cloud is commonly called the surface reconstruction problem, although this might also incorporate reconstruction of other complete surface representations. The most powerful algorithm to deal with mesh construction given a point cloud is the *power crust* algorithm, described in Amenta et al. (2001). Other algorithms that deal with this problem are, a.o., the algorithms of Hoppe et al. (1992), Edelsbrunner & Mücke (1994) and Curless & Levoy (1996). A short overview of methods for triangulation can be found in the paper of Varshosaz et al. (2005).

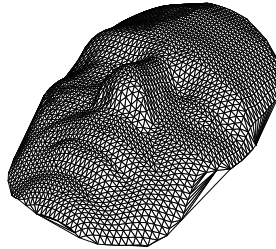


Fig. 5. An example of a 3D face represented as a mesh.

Probably the main benefit of a polygon mesh is its ease of visualization. Many algorithms for ray tracing, collision detection, and rigid-body dynamics are developed for polygon meshes. Another advantage of meshes, certainly in comparison to point clouds, is the explicit knowledge of connectivity, which is useful for the computation of the geodesic distance between two points. This is particularly useful in face recognition because geodesic distances between points on the surface are often used in 3D expression-invariant face recognition, because they seem to vary less than Euclidean distances. The use of this was introduced by Bronstein et al. (2003), using a fast marching method for triangulated domains (Kimmel & Sethian, 1998) for geodesic distance calculation. Afterwards, many other researchers used the concept of invariance of geodesic distances during expression variations, by directly comparing point wise distances (Gupta et al., 2007; Li & Zhang, 2007; Smeets et al., 2009) or using iso-geodesic curves (see section 2.2). On the other hand, mesh errors like cracks, holes, T-joints, overlapping polygons, duplicated geometry, self intersections and inconsistent normal orientation can occur as described by Veleba & Felkel (2007).

2.4 Parametric surface representations

A generic parametric form for representing 3D surfaces is a function with domain \mathbb{R}^2 and range \mathbb{R}^3 (Campbell & Flynn, 2000):

$$\mathcal{S}(u, v) = \begin{cases} x = f_1(u, v) \\ y = f_2(u, v) \\ z = f_3(u, v) \end{cases} \quad (1)$$

where u and v are the two parametric variables.

Amongst the advantages of parametric representations in general we can count the simple but general and complete mathematical description, the easiness to handle and the readiness of technology to visualise these representations. General disadvantages are that only functions can be represented, which cause problems in, for instance, the ear and nose regions.

The class of parametric surface representations is very general, but the following three deserve particular attention.

2.4.1 Height maps

A height map is a special form of a parametric surface with $x = u$ and $y = v$ and is also often referred as depth map, range image or graph surface. A height map represents the height of points along the z -directions in a regular sampling of the x, y image axes in a matrix. An example of a face represented as a depth map can be seen in figure 6. A big advantage of this representation is that many 3D laser scanners produce this kind of output. Because mostly the x and y values lay on a regular grid, the surface can be described by a matrix and 2D image processing techniques can be applied on it. The most prominent disadvantage of height maps is the limited expressional power: only what is 'seen' when looking from one direction (with parallel beams) can be represented. This causes problems in the representation of, for instance, the cheeks and ears of human faces. The use of height maps in face recognition has already been discussed by Akarun et al. (2005). One very specific example of a 3D face recognition method using height maps is the method of Samir et al. (2006), because here height maps are extracted from triangulated meshes in order to represent the surface by level curves, which are iso-contours of the depth map. Colbry & Stockman (2007) extend the definition of depth map leading to the canonical face depth map. This is obtained by translating a parabolic cylinder or a quadratic, instead of a plane, along the z -direction. Because of this alternative definition, it could also belong to section 2.4.2.



Fig. 6. An example of a height map surface representation.

2.4.2 Geometry images

Another often used parametric surface representation is the geometry image, a regularly sampled 2D grid representation, but here not representing the distance to the surface along a viewing direction. The directions are 'adaptive' in the sense that they are conveyed so to be able to represent the whole surface, thus also regions that would not be representable in a height map due to the directionality of 'height'. Gu et al. (2002) describe an automatic system for converting arbitrary meshes into geometry images: the basic idea is to slice open the mesh along an appropriate selection of cut paths in order to unfold the mesh. Next the cut surface is parametrized onto a square domain containing this opened mesh creating an $n \times n$ matrix of $[x, y, z]$ data values. The geometry image representation has some advantages, the biggest being that the irregular surface is represented on a completely regular grid, without losing information. As with the height map, this structure is easy to process, both for graphics applications and for recognition applications. A big disadvantage is the computational and technical complexity of the generation of geometry images.

Geometry images have already been used for 3D face recognition. In (Kakadiaris et al., 2007; Perakis et al., 2009), a geometry image maps all vertices of the face model surface from \mathbb{R}^3 to \mathbb{R}^2 . This representation is segmented to form the Annotated Face Model (AFM) which is rigidly aligned with the range image of a probe. Afterwards, the AFM is fitted to each probe data set using the elastically adapted deformable model framework, described by Metaxas & Kakadiaris (2002). The deformed model is then again converted to a geometry image and a normal map. Those images are analysed using the Haar and pyramid wavelet transform. The distance metric that is used to compare different faces, uses the coefficients of the wavelet transforms.

2.4.3 Splines

Spline surfaces are piecewise polynomial parametric surface representations that are very popular in the field of Computer Aided Design and Modelling (CAD/CAM) because of the simplicity of their construction, including interpolation and approximation of complex shapes, and their ease and accuracy of evaluation. The basis of splines are control points, which are mostly lying on a regular grid.

One well-known type of spline surfaces are Bézier surfaces. These are represented as:

$$S(u, v) = \sum_{i=0}^n \sum_{j=0}^m B_i^n(u) B_j^m(v) \vec{x}_{i,j} \quad (2)$$

where B_i^n are Bernstein polynomials. Another well-known spline surface type are nonuniform rational B-splines (NURBS), defined as

$$S(u, v) = \sum_{i=1}^k \frac{N_{i,n} w_i}{\sum_{j=1}^k N_{j,n} w_j} \vec{x}_i, \quad (3)$$

with k the number of control points \vec{x}_i and w_i the corresponding weights. An example of face representation by Bézier curves can be found in (Yang et al., 2006) and of NURBS in (Liu et al., 2005; Yano & Harada, 2007). Although spline surfaces have been considered for representing faces, they have not found widespread use in 3D face recognition. Most probably because, as is stated by Besl (1990), a.o.: "it is difficult to make a surface defined on a parametric rectangle fit an arbitrary region on the surface". Also, the control points are not easily detectable. Another disadvantage of splines is the uselessness of the spline parameters for recognition.

2.5 Spherical harmonics surface representations

Spherical harmonics are mathematical functions that can be used for representing spherical objects (sometimes also called star-shaped objects). The surface first has to be represented as a function on the unit sphere: $f(\theta, \phi)$. This function can then be decomposed (spherically expanded) as:

$$f(\theta, \phi) = \sum_{l=0}^{\infty} \sum_{m=-l}^l a_{lm} Y_l^m(\theta, \phi). \quad (4)$$

The spherical harmonics $Y_l^m(\theta, \phi) : |m| \in \mathbb{N}$ are defined on the unit sphere as:

$$Y_l^m(\theta, \phi) = k_{l,m} P_l^m(\cos \theta) e^{im\phi}, \quad (5)$$

where $\theta \in [0, \pi]$, $\phi \in [0, 2\pi[$, $k_{l,m}$ is a constant, and P_l^m is the associated Legendre polynomial. The coefficients a_{lm} are uniquely defined by:

$$a_{lm} = \int_0^{2\pi} \int_0^{\pi} f(\theta, \phi) \overline{Y_l^m(\theta, \phi)} \sin(\theta) d\theta d\phi. \quad (6)$$

While this theory is stated for spherical objects, it is important to mention that spherical harmonics have already been used for non spherical objects by first decomposing the object into spherical subparts (Mousa et al., 2007) using the volumetric segmentation method proposed by Dey et al. (2003).

Advantages of the spherical harmonics surface representation include the similarity to the Fourier transform, which has already proven to be a very interesting technique in 1D signal processing. Also, because of the spectral nature of this surface representation, it can lead to large dimensionality reductions, leading to decreases in computation time and efficient storage. Other advantages are the rotational invariance of the representation and the ability to cope with missing data (occlusions and partial views).

The spherical harmonics surface representation has some drawbacks as well. One of them has already been mentioned and is not insuperable: the need for spherical surfaces. Other disadvantages include the unsuitability for intuitive editing, the non-trivial visualisation and the global nature of the representation.

Spherical harmonics surface representations have already been used in a number of applications that bear a close relation to face recognition. Kazhdan et al. (2003) used it as a 3D shape descriptor for use in searching a 3D model database. Mousa et al. (2007) use the spherical harmonics for reconstruction of 3D objects from point sets, local mesh smoothing and texture transfer. Dillenseger et al. (2006) have used it for 3D kidney modelling and registration. To the best of our knowledge, the only use of this representation in face recognition so far is in (Llonch et al., 2009). In this work, a similar transformation with another (overcomplete) basis is used as a surface representation for the 3D faces in the face recognition experiments, where this representation is also submitted to linear discriminant analysis (LDA). The performance reported is better than PCA on depth maps, which the authors consider as baseline.

Further applications in face recognition are not yet widely explored, but we see a great potential in the method of Bülow & Daniilidis (2001), who combine the spherical harmonics representation with Gabor wavelets on the sphere. In this way, the main structure of the 3D face is represented globally, while the (person-specific) details are modelled locally (with wavelets). This solves the drawback of the global nature of the representation and could as such be used for multiscale progressive 3D face recognition.

2.6 Point cloud-based surface representations: information theoretic measures

Recently, some researchers have proposed to work directly on the point cloud, without using any real surface representation, but instead use information theoretic measures defined directly on the raw point cloud surface representation. Some of these methods do nevertheless implicitly use some kind of kernel surface representation, which can also be viewed as density estimation (Silverman, 1986), and although the density estimation itself is explicit, the surface can be thought of as implicitly present. This is also the reason why this surface representation was not included in section 2.1 (which would also make sense) but is treated as a link between the explicit and implicit surface representations. Density estimation is a fundamental concept in statistics, the search for an estimate of the density from a given dataset. In the case of surface representations, this dataset is a point cloud. This estimation can be nonparametric, which can be considered as an advantage of this method. Also the generality, sound statistical base and low data requirements are advantages. Disadvantages include the difficulties in visualising the surface representation,

The most used density estimation technique is kernel density estimation KDE, introduced by Parzen (1962). Here the density is computed as

$$\hat{f}_h(\vec{x}) = \frac{1}{nh} \sum_{i=1}^n K\left(\frac{\vec{x} - \vec{x}_i}{h}\right) \quad (7)$$

where K is some kernel with parameter h . A volume rendering of a KDE of a 3D face surface can be seen in figure 7.

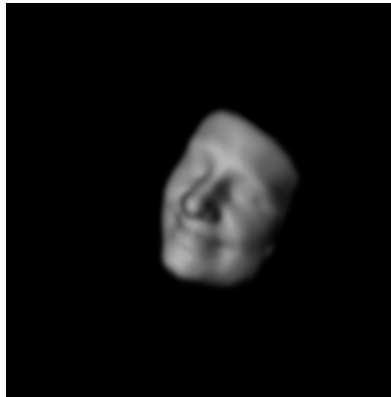


Fig. 7. Volume rendering of a kernel density estimation of a human face.

The information theoretic methods have already been proven to be useful in 3D registration and recognition. Tsin & Kanade (2004) proposed the *kernel correlation* of two point clouds, an entropy-related measure expressing the compatibility of two point clouds, and used this for robust 3D registration. This measure has later been used in 3D face recognition by Fabry et al. (2008). A related technique, which has until now not been applied to face recognition, is found in (Wang et al., 2008). Here, groupwise registration between point clouds is performed by minimizing the Jensen-Shannon divergence between the Gaussian mixture representations of the point clouds.

3. Implicit surface representations

In general, implicit functions are defined as the iso-level of a scalar function $\phi : \mathbb{R}^n \rightarrow \mathbb{R}$. A 3D implicit surface \mathcal{S} is then mathematically defined as

$$\mathcal{S} = \{\vec{x} \in \mathbb{R}^3 | \phi(\vec{x}) = \rho\}. \quad (8)$$

We call this the *iso-surface* of the implicit function. The iso-surface at $\rho = 0$ is sometimes referred to as the *zero contour* or *zero surface*. As such, implicit surfaces are 2D geometric shapes that exist in 3D space (Bloomenthal & Wyvill, 1997). The iso-surface partitions the space into two regions: interior of the surface, and exterior of the surface. Mostly, the convention is followed that inside the surface, the function returns negative values and outside the surface, the function returns positive values. The inside portion is referred as Ω^- , while points with positive values belong to the outside portion Ω^+ . The border between the inside and the outside is called the interface $\partial\Omega$.

The simplest surfaces (spheroids, ellipsoids,...) can be described by analytic functions and are called algebraic surfaces. The surface is the set of roots of a polynomial $\phi(\vec{x}) = \rho$. The degree of the surface n is the maximum sum of powers of all terms. The general form of a linear surface ($n = 1$), or plane, is

$$\phi(x, y, z) = ax + by + cz - d = \rho, \quad (9)$$

while the general form for a quadratic surface ($n = 2$) is:

$$\begin{aligned} \phi(x, y, z) &= ax^2 + bxy + cxz + dx + ey^2 + fyz + gy + hz^2 + iz + j \\ &= \rho. \end{aligned} \quad (10)$$

Superquadrics ($n > 2$) provide more flexibility by adding parameters to control the polynomial exponent, allowing to describe more complex surfaces. Nevertheless, analytic functions are designed to describe a surface globally by a single closed formula. In reality, it is mostly not possible to represent a whole real-life object by an analytic function of this form.

3.1 Radial Basis Functions

Radial Basis Functions (RBFs) are another type of implicit functions that have been proven to be a powerful tool in interpolating scattered data of all kinds, including 3D point clouds representing 3D objects. A RBF is a function of the form

$$\mathcal{S}(\vec{x}) = \sum_{i=1}^N \lambda_i \Phi(\|\vec{x} - \vec{x}_i\|) + p(\vec{x}), \quad (11)$$

with λ_i the *RBF-coefficients*, Φ a *radial basic function*, \vec{x}_i the *RBF centra* and $p(\vec{x})$ a polynomial of low degree.

As can be seen from equation (11), the RBF consists of a weighted sum of radially symmetric basic functions located at the RBF-centra x_i and a low degree polynomial p . For surface representation, the RBF-centra x_i are simply a subset of points on the surface. Finding the appropriate RBF-coefficients for implicitly representing a surface is done by solving:

$$\forall x_i : s(x_i) = f_i, \quad (12)$$

For a surface representation, we want the surface to be the zero-contour of the implicit surface $s(\vec{x})$ and hence $f_i = 0, \forall i$. To prevent the interpolation to lead to the trivial solution, $s(\vec{x}) = 0$ everywhere, we have to add additional constraints. This is done by adding *off-surface points*: points at a distance of the surface, whose implicit function value is different from zero and mostly equal to the euclidean distance to the surface. Figure 8 gives an example of a RBF interpolation with zero iso-surface.

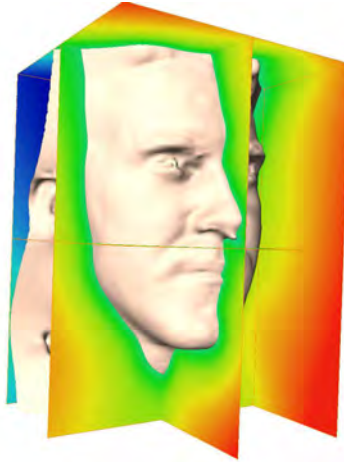


Fig. 8. An example of a RBF interpolation with zero iso-surface.

A very clear introduction to the RBF-theory, and info about a fast commercial RBF-implementation can be found in (Far, 2004). A mathematically very complete reference book about Radial Basis Functions is (Buhmann, 2003).

The biggest advantage of radial basis function interpolation is the absence of the need for point connectivity. Other advantages include the low input data requirements (bare point clouds), and the possibility to insert smoothness constraints when solving for the RBF. A disadvantage of RBFs is the computational complexity of the problem. This problem can however be alleviated by specific mathematical algorithms (Fast Multipole Methods (Beatson & Greengard, 1997)), or compactly supported basis functions (Walder et al., 2006). Because of this computational complexity, also the editing of the surface is not trivial.

In Claes (2007), a robust framework for both rigid and non-rigid 3D surface representation is developed to represent faces. This application can be seen as 3D face biometrics in the wide sense: representing and distinguishing humans by measuring their *face geometry*. This is used for craniofacial reconstruction.

Thin Plate Splines, one particular kind of RBF basic function, are popular in non-rigid registration of face models. Surface registration is an important step in some model-based 3D face recognition methods, but then the RBF is not used as the surface representation method but merely as a preprocessing technique (Irfanoglu et al., 2004; Lu & Jain, 2005).

Another application of RBFs in face recognition can be found in (Pears, 2008), where the RBF is sampled along concentric spheres around certain landmarks to generate features for face recognition.

3.2 Blobby Models

The blobby model is another kind of implicit surface representation introduced by Blinn (1982). It was originally perceived as a way to model molecular models for display, and is, as such, tightly related to the quantum mechanical representation of an electron: a density function of the spatial location. This way, the molecule surface can be thought of as the ρ iso-contour of the sum of atom contributions

$$D(x, y, x) = \sum_i b_i \exp(-a_i r_i^2), \quad (13)$$

where r_i are distances to the atom locations. Various variants of the original blobby models exist, which can also be called *metaballs* or *soft objects*, and instead of the exponential, one can also use polynomials (Nishita & Nakamae, 1994) or ellipsoids (Liu et al., 2007) to represent the blobs.

An advantage of the blobby model surface representation is the apparent possibility for huge data reduction without loosing much detail. However, the efficient construction of blobby models is still a problem under research (Liu et al., 2007).

Maruki Muraki (1991) used this blobby model to describe a surface originally represented by range data with normals. He does this by solving an optimization problem with parameters x_i, y_i, z_i, a_i, b_i with x_i, y_i, z_i the locations of the blobs and a_i, b_i the blob parameters. Interestingly, the examples shown in this 1991 paper are representations of faces. It seems that a face can reasonably well be represented with about 250 blobs, making this representation promising for 3D face recognition.

Nevertheless, there are not yet applications of this method in 3D face recognition. It has however been used in the related problem of *natural object recognition*, where 2D contours were represented as blobby models, and these blobby models were then used for classification of the contours (Jorda et al., 2001).

3.3 Euclidean distance functions

A special class of scalar functions are distance functions. The *unsigned distance function* yields the distance from a point \vec{p} to the closest point on the surface \mathcal{S} (Jones et al., 2006):

$$dist_{\mathcal{S}}(\vec{p}) = \inf_{\vec{x} \in \mathcal{S}} \|\vec{x} - \vec{p}\|, \quad (14)$$

while *signed distance functions* represent the same, but have a negative sign in Ω^- , inside the object. The signed distance function is constructed by solving the Eikonal equation:

$$\|\nabla\phi(x, y, z)\| = 1, \quad (15)$$

together with the boundary condition $\phi|_{\mathcal{S}} = 0$. At any point in space, ϕ is the Euclidean distance to the closest point on \mathcal{S} , with a negative sign on the inside and a positive on the outside (Sigg, 2006). The gradient is orthogonal to the iso-surface and has a unit magnitude (Jones et al., 2006). An example of a distance function is given in figure 9. The signed distance function can also be approximated using Radial Basis Functions (Far, 2004), as shown in figure 8.

One advantage of a surface represented by a distance function is that the surface can easily be evolved using a level set method. In those methods, also other implicit surface representations are possible, but distance transforms have nice numerical properties (Osher & Fedkiw, 2003).

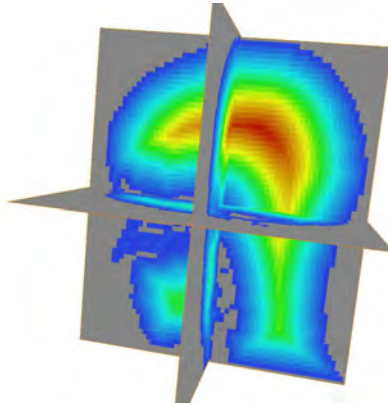


Fig. 9. An example of a distance function.

An interesting application in face recognition (in 2D though) is given in (Akhloufi & Bendada, 2008) where a distance transform is used to get an invariant representation for face recognition, using thermal face images. After extraction of the face region, a clustering technique constructs the facial isotherm layers. Computing the medial axis in each layer provides an image containing physiological features, called face print image. A Euclidean distance transform provides the necessary invariance in the matching process. Related to the domain of face recognition, the signed distance function is used in craniofacial reconstruction (Vandermeulen et al., 2006). A reference skull, represented as distance maps, is warped to all target skulls and subsequently these warps are applied to the reference head distance map.

Signed distance maps are also interesting for aligning surfaces, as described in Hansen et al. (2007). Symmetric registration of two surfaces, represented as signed distance maps, is done by minimizing the energy functional:

$$\begin{aligned}
 F(\vec{p}) = & \sum_{\vec{x} \in U_x^r} (\phi_y(W(\vec{x}; \vec{p})) - \phi_x(\vec{x}))^2 \\
 & + \sum_{\vec{y} \in U_y^r} (\phi_x(W(\vec{y}; \vec{p})) - \phi_y(\vec{y}))^2,
 \end{aligned} \tag{16}$$

with $W(-; \vec{p})$ the warp function, U_x^r and U_y^r the narrow bands around the surfaces S_x and S_y and ϕ the signed distance map. The width of the narrow band r should be larger than the width of the largest structure. Hansen et al. (2007) state that the level set registration performs slightly better than the standard ICP algorithm (Besl & McKay, 1992).

3.4 Random walk functions

This scalar surface representation gives at a point in space a value that is the average time of a random walk to reach the surface starting from that point. This scalar function is the result of solving the Poisson equation:

$$\Delta\phi(x, y, z) = -1, \tag{17}$$

again subject to the boundary condition $\phi|_S = 0$ and with $\Delta\phi = \frac{\partial^2\phi}{\partial x^2} + \frac{\partial^2\phi}{\partial y^2} + \frac{\partial^2\phi}{\partial z^2}$. For every internal point in the surface, the function assigns a value reflecting the mean time required for

a random walk beginning at the boundaries and ending in this particular point. The level sets of ϕ represent smoother versions of the bounding surface. A disadvantage of this function is that a unique solution of equation (17) only exists within a closed surface. An example of a random walk function is given in figure 10.

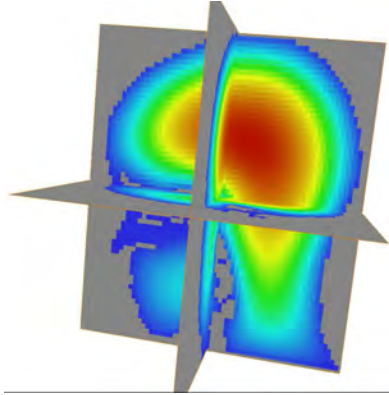


Fig. 10. An example of a random walk function.

To the best of our knowledge, this scalar function is not yet used in face recognition. However, it has already been proven to be useful in 2D object classification which makes it for auspicious for use in biometrics (Gorelick et al., 2006).

4. Conclusions

We can conclude that, although many representations in biometrics are based on meshes, a number of interesting alternatives exist. We have given a systematic discussion of the different three-dimensional surface representations that seem to be promising for use in 3D biometrics and, if known, their already existing use. While we are aware of the non-exhaustive nature of this work, we hope to have given to the face recognition and other related research communities (computer graphics, mathematics of surfaces, . . .) some interesting ideas.

We have paid attention to the advantages and disadvantages of the different surface representations throughout the whole text. The main advantages and disadvantages of the different surface representations are summarized in table 1. From this we can conclude that many of the advantages of the different surface representations have not yet been taken advantage of in current face recognition research. This could thus be very interesting for future research.

Other interesting conclusions can be drawn from the preceding text and table. First of all, we see that the left branch of our taxonomy, the explicit representations, is much more frequently used in today's face recognition research, opposed to the other branch, the implicit representations. This can be explained by the fact that explicit representations have been very much a topic of interest in computer graphics because of hardware requirements and are as such also the first to be considered in 3D face recognition.

Furthermore: although the polygonal mesh is often used in 3D face recognition and certainly has some advantages, we think it is more important to keep the other surface representations in mind for doing face recognition research. Moreover, we already see a gain in importance of meshfree methods in the field of numerical analysis, where meshfree methods are used

	Accuracy	Conciseness	Acquiring	Intuitiveness	Parameterization	Computability	Displayability	Main advantage	Main disadvantage	Previous use in face recognition
Point Cloud	±	±	+	+	±	+	+	Simplicity	Sparseness	many (see text)
Contour and profile curves	-	+	±	+	+	±	+	Invariance	Sparseness	many (see text)
Polygonal Mesh	+	±	±	+	±	±	+	Many tools	Discrete	many (see text)
Parametric										
• Height map	±	±	+	±	+	+	±	Aquiring	Self Occlusion	many (see text)
• Geometry image	+	±	-	-	+	±	±	Parameterization	Construction	Metaxas & Kakadiaris (2002)
• Splines	+	+	-	±	+	+	+	Parameterization	Computability	not yet...
Spherical harmonics	+	+	-	-	+	-	-	Multiresolution	Globality	Llorch et al. (2009)
Point-Cloud based	±	±	-	±	±	-	-	Sound theory	Computability	Fabry et al. (2008)
Radial Basis Functions	+	±	-	±	+	-	-	Completeness	Computability	not yet...
Blobby Models	+	+	-	±	+	-	-	Compression	Construction	not yet...
Distance Functions	+	-	-	±	±	-	-	Evolution	Memory req.	not yet...
Random walk function	+	-	-	±	±	-	-	Evolution	Memory req.	not yet...

Table 1. Summary of advantages and disadvantages of the discussed surface representations.

in finite element modelling, for solving partial differential equations or for approximating functions without using classic mesh discretisations. These kind of methods have many advantages: easy handling of large deformations because of the lack of connectivity between points, good handling of topological changes, ability to include prior knowledge, support for flexible adaptable refinement procedures, the ability to support multiscale... (Li & Liu, 2004). Also in computer graphics, meshfree surface representations are gaining importance, especially in the physically based deformable models (Nealen et al., 2006), but also in many other computer graphics subfields (Dyn et al., 2008; Sukumar, 2005). In 3D face recognition, some progressive methods make use of some of these interesting meshfree surface representations as explained in this chapter.

5. References

- Akarun, L., Gokberk, B. & Salah, A. A. (2005). 3D face recognition for biometric applications, *EUSIPCO '05: Proceedings of the 13th European Signal Processing Conference*, Antalya.
- Akhoulfi, M. & Bendada, A. H. (2008). Infrared face recognition using distance transforms, *ICIVC 2008: International Conference on Image and Vision Computing*, Vol. 30 of *Proceedings of World Academy of Science, Engineering & Technology*, Paris, France, pp. 160–163.
- Al-Osaimi, F., Bennamoun, M. & Mian, A. (2009). An expression deformation approach to non-rigid 3D face recognition, *International Journal of Computer Vision* **81**(3): 302–316.
- Alyüz, N., Gökberk, B. & Akarun, L. (2008). A 3D face recognition system for expression and occlusion invariance, *BTAS '08: Proceedings of the IEEE Second International Conference on Biometrics Theory, Applications and Systems*, Arlington, Virginia, USA.
- Amberg, B., Knothe, R. & Vetter, T. (2008). Expression invariant 3D face recognition with a morphable model, *FG '08: Proceedings of the 8th IEEE International Conference on Automatic Face and Gesture Recognition*, IEEE Computer Society, Amsterdam, The Netherlands.
- Amenta, N., Choi, S. & Kolluri, R. K. (2001). The power crust, *SMA '01: Proceedings of the sixth ACM symposium on Solid modeling and applications*, ACM, New York, NY, USA, pp. 249–266.
- Beatson, R. & Greengard, L. (1997). A short course on fast multipole methods, *Wavelets, Multilevel Methods and Elliptic PDEs*, Oxford University Press, pp. 1–37.
- Berretti, S., Bimbo, A. D. & Pala, P. (2006). Description and retrieval of 3D face models using iso-geodesic stripes, *MIR '06: Proceedings of the 8th ACM international workshop on Multimedia information retrieval*, ACM, New York, NY, USA, pp. 13–22.
- Besl, P. (1990). The free-form surface matching problem, *Machine vision for three-dimensional scenes* pp. 25–71.
- Besl, P. J. & McKay, N. D. (1992). A method for registration of 3-D shapes, *IEEE Transactions on Pattern Analysis and Machine Intelligence* **14**(2): 239–256.
- Blinn, J. F. (1982). A generalization of algebraic surface drawing, *ACM Trans. Graph.* **1**(3): 235–256.
- Bloomenthal, J. & Wyvill, B. (eds) (1997). *Introduction to Implicit Surfaces*, Morgan Kaufmann Publishers Inc., San Francisco, CA, USA.
- Bronstein, A. M., Bronstein, M. M. & Kimmel, R. (2003). Expression-invariant 3D face recognition, in J. Kittler & M. Nixon (eds), *AVBPA '03: Proceedings of the 4th International Conference on Audio and Video-based Biometric Person Authentication*, Vol. 2688 of *Lecture Notes in Computer Science*, Springer, pp. 62–69.

- Bronstein, A. M., Bronstein, M. M. & Kimmel, R. (2005). Three-dimensional face recognition, *International Journal of Computer Vision* **64**(1): 5–30.
- Buhmann, M. (2003). *Radial Basis Functions: Theory and Implementations*, Cambridge University Press.
- Bülöw, T. & Daniilidis, K. (2001). Surface representations using spherical harmonics and gabor wavelets on the sphere, *Technical Report MS-CIS-01-37*, University of Pennsylvania, Department of Computer and Information Science.
- Campbell, R. J. & Flynn, P. J. (2000). Survey of free-form object representation and recognition techniques, *Computer Vision and Image Understanding* **81**: 166–210.
- Chang, K. I., Bowyer, K. W. & Flynn, P. J. (2006). Multiple nose region matching for 3D face recognition under varying facial expression, *IEEE Transactions on Pattern Analysis and Machine Intelligence* **28**(10): 1695–1700.
- Claes, P. (2007). *A robust statistical surface registration framework using implicit function representations - application in craniofacial reconstruction*, PhD thesis, Katholieke Universiteit Leuven, Leuven, Belgium.
URL: <http://www.medicalimagingcenter.be/PhD/PeterClaes/Thesis.pdf>
- Colbry, D. & Stockman, G. C. (2007). Canonical face depth map: A robust 3D representation for face verification, *CVPR '07: Proceedings of the IEEE Computer Society Conference on Computer Vision and Pattern Recognition*, IEEE Computer Society, Minneapolis, Minnesota, USA.
- Curless, B. & Levoy, M. (1996). A volumetric method for building complex models from range images, *SIGGRAPH '96: Proceedings of the 23rd annual conference on Computer graphics and interactive techniques*, ACM, New York, NY, USA, pp. 303–312.
- Dey, T., Giesen, J. & Goswami, S. (2003). Shape segmentation and matching with flow discretization, *Algorithms and Data Structures* pp. 25–36.
URL: <http://www.springerlink.com/content/6qwfh2adqmm60n30>
- Dillenseger, J.-L., Guillaume, H. & Patard, J.-J. (2006). Spherical harmonics based intrasubject 3-d kidney modeling/registration technique applied on partial information, *Biomedical Engineering*, *IEEE Transactions on* **53**(11): 2185–2193.
- Dyn, N., Iske, A. & Wendland, H. (2008). Meshfree thinning of 3d point clouds, *Foundations of Computational Mathematics* **8**(4): 409–425.
- Edelsbrunner, H. & Mücke, E. P. (1994). Three-dimensional alpha shapes, *ACM Trans. Graph.* **13**(1): 43–72.
- Fabio, R. (2003). From point cloud to surface: the modeling and visualization problem, *Workshop on Visualization and Animation of Reality-based 3D Models*, Tarasp-Vulpera, Switzerland.
- Fabry, T., Vandermeulen, D. & Suetens, P. (2008). 3D face recognition using point cloud kernel correlation, *BTAS '08: Proceedings of the IEEE Second International Conference on Biometrics Theory, Applications and Systems*, Arlington, Virginia, USA.
- Faltemier, T., Bowyer, K. W. & Flynn, P. J. (2008). A region ensemble for 3-D face recognition, *IEEE Transactions on Information Forensics and Security* **3**(1): 62–73.
- Far (2004). *FastRBF MATLAB Toolbox Manual*.
- Feng, S., Krim, H., Gu, I. & Viberg, M. (2006). 3D face recognition using affine integral invariants, *ICASSP '06: Proceedings of the IEEE International Conference on Acoustics, Speech and Signal Processing*, Vol. 2, Toulouse, France, pp. 189–192.

- Feng, S., Krim, H. & Kogan, I. A. (2007). 3D face recognition using euclidean integral invariants signature, *SSP '07: IEEE/SP 14th Workshop on Statistical Signal Processing*, Madison, WI, USA, pp. 156–160.
- Gorelick, L., Galun, M. & Brandt, A. (2006). Shape representation and classification using the poisson equation, *IEEE Transactions on Pattern Analysis and Machine Intelligence* **28**(12): 1991–2005. Member-Eitan Sharon and Member-Ronen Basri.
- Gu, X., Gortler, S. J. & Hoppe, H. (2002). Geometry images, *ACM Trans. Graph.* **21**(3): 355–361.
- Gupta, S., Aggarwal, J. K., Markey, M. K. & Bovik, A. C. (2007). 3D face recognition founded on the structural diversity of human faces, *CVPR '07: Proceedings of the International Conference on Computer Vision and Pattern Recognition*, IEEE Computer Society, Minneapolis, Minnesota, USA.
- Hansen, M. F., Erbou, S. G. H., Vester-Christensen, M., Larsen, R., Ersboll, B. K. & Christensen, L. B. (2007). Surface-to-surface registration using level sets, in B. K. Ersboll & K. S. Pedersen (eds), *SCIA '07: Proceedings of the 15th Scandinavian Conference on Image Analysis*, Vol. 4522 of *Lecture Notes in Computer Science*, Springer, pp. 780–788.
- Hoppe, H., DeRose, T., Duchamp, T., McDonald, J. & Stuetzle, W. (1992). Surface reconstruction from unorganized points, *SIGGRAPH '92: Proceedings of the 19th annual conference on Computer graphics and interactive techniques*, ACM, New York, NY, USA, pp. 71–78.
- Hubeli, A. & Gross, M. (2000). A survey of surface representations for geometric modeling, *Technical Report 335*, ETH Zürich.
- Irfanoglu, M., Gokberk, B. & Akarun, L. (2004). 3D shape-based face recognition using automatically registered facial surfaces, *Pattern Recognition, 2004. ICPR 2004. Proceedings of the 17th International Conference on* **4**: 183–186 Vol.4.
- Jahanbin, S., Choi, H., Liu, Y. & Bovik, A. C. (2008). Three dimensional face recognition using iso-geodesic and iso-depth curves, *BTAS '08: Proceedings of the IEEE Second International Conference on Biometrics Theory, Applications and Systems*, Arlington, Virginia, USA.
- Jones, M. W., Baerentzen, J. A. & Sramek, M. (2006). 3D distance fields: A survey of techniques and applications, *IEEE Transactions on Visualization and Computer Graphics* **12**(4): 581–599.
- Jorda, A. R., Vanacloig, V. A. & García, G. A. (2001). A geometric feature set based on shape description primitives to recognize natural objects, *Proceedings of the IX Spanish Symposium on Pattern Recognition and Image Analysis*, Benicasim, Spain.
- Kakadiaris, I. A., Passalis, G., Toderici, G., Murtuza, M. N., Lu, Y., Karampatziakis, N. & Theoharis, T. (2007). Three-dimensional face recognition in the presence of facial expressions: An annotated deformable model approach, *IEEE Transactions on Pattern Analysis and Machine Intelligence* **29**(4): 640–649.
- Kalaiah, A. & Varshney, A. (2003). Statistical point geometry, *SGP '03: Proceedings of the 2003 Eurographics/ACM SIGGRAPH symposium on Geometry processing*, Eurographics Association, pp. 107–115.
- Kazhdan, M., Funkhouser, T. & Rusinkiewicz, S. (2003). Rotation invariant spherical harmonic representation of 3d shape descriptors, *SGP '03: Proceedings of the 2003 Eurographics/ACM SIGGRAPH symposium on Geometry processing*, Eurographics Association, Aire-la-Ville, Switzerland, Switzerland, pp. 156–164.
- Kimmel, R. & Sethian, J. A. (1998). Computing geodesic paths on manifolds, *Proceedings of the National Academy of Sciences of the United States of America* **95**: 8431–8435.

- Levoy, M. & Whitted, T. (1985). The use of points as a display primitive, *Technical report*, Department of Computer Science, University of North Carolina at Chappel Hill.
- Li, L., Xu, C., Tang, W. & Zhong, C. (2008). 3d face recognition by constructing deformation invariant image, *Pattern Recognition Letters* **29**(10): 1596–1602.
- Li, S. & Liu, W. (2004). *Meshfree particle methods*, Springer.
- Li, X. & Zhang, H. (2007). Adapting geometric attributes for expression-invariant 3D face recognition, *SMI '07: Proceedings of the IEEE International Conference on Shape Modeling and Applications*, IEEE Computer Society, Washington, DC, USA, pp. 21–32.
- Liu, D., Shen, L. & Lam, K. (2005). Image Synthesis and Face Recognition Based on 3D Face Model and Illumination Model, *ICNC 2005*, Springer, p. 7.
- Liu, S., Jin, X., Wang, C. & Hui, K. (2007). Ellipsoidal-blob approximation of 3D models and its applications, *Computers & Graphics* **31**(2): 243–251.
- Llonch, R. S., Kokkiopoulou, E., Tomic, I. & Frossard, P. (2009). 3D face recognition with sparse spherical representations, *Pattern Recognition*.
- Lu, X. & Jain, A. K. (2005). Deformation analysis for 3d face matching, *WACV-MOTION '05: Proceedings of the Seventh IEEE Workshops on Application of Computer Vision (WACV/MOTION'05) - Volume 1*, IEEE Computer Society, Washington, DC, USA, pp. 99–104.
- Lu, X. & Jain, A. K. (2006). Deformation modeling for robust 3D face matching, *CVPR '06: Proceedings of the 2006 IEEE Computer Society Conference on Computer Vision and Pattern Recognition*, IEEE Computer Society, Washington, DC, USA, pp. 1377–1383.
- Marr, D. (1982). *Vision: a computational investigation into the human representation and processing of visual information*, W. H. Freeman, San Francisco.
- Maurer, T., Guignonis, D., Maslov, I., Pesenti, B., Tsaregorodtsev, A., West, D. & Medioni, G. (2005). Performance of Geometrix ActiveIDTM 3D face recognition engine on the FRGC data, *CVPR '05: Proceedings of the 2005 IEEE Computer Society Conference on Computer Vision and Pattern Recognition (CVPR'05) - Workshops*, IEEE Computer Society, Washington, DC, USA, p. 154.
- Metaxas, D. N. & Kakadiaris, I. A. (2002). Elastically adaptive deformable models, *IEEE Transactions on Pattern Analysis and Machine Intelligence* **24**(10): 1310–1321.
- Mousa, M.-H., Chaine, R., Akkouche, S. & Galin, E. (2007). Efficient spherical harmonics representation of 3d objects, *PG '07: Proceedings of the 15th Pacific Conference on Computer Graphics and Applications*, IEEE Computer Society, Washington, DC, USA, pp. 248–255.
- Mpiperis, I., Malasiotis, S. & Strintzis, M. G. (2007). 3-D face recognition with the geodesic polar representation, *IEEE Transactions on Information Forensics and Security* **2**(3): 537–547.
- Mpiperis, I., Malasiotis, S. & Strintzis, M. G. (2008). Bilinear models for 3-D face and facial expression recognition., *IEEE Transactions on Information Forensics and Security* **3**(3): 498–511.
- Muraki, S. (1991). Volumetric shape description of range data using “blobby model”, *SIG-GRAPH Comput. Graph.* **25**(4): 227–235.
- Nealen, A., Mueller, M., Keiser, R., Boxerman, E. & Carlson, M. (2006). Physically based deformable models in computer graphics, *Computer Graphics Forum* **25**(4): 809–836.
URL: <http://dx.doi.org/10.1111/j.1467-8659.2006.01000.x>
- Nishita, T. & Nakamae, E. (1994). A method for displaying metaballs by using bezier clipping, *Computer Graphics Forum* **13**: 271–280.

- Osher, S. & Fedkiw, R. (2003). *Level Set Methods and Dynamic Implicit Surfaces*, Vol. 153 of *Applied Mathematical Sciences*, Springer-Verlag New York.
- Parzen, E. (1962). On estimation of a probability density function and mode, *The Annals of Mathematical Statistics* **33**(3): 1065–1076.
URL: <http://www.jstor.org/stable/2237880>
- Pauly, M., Keiser, R. & Gross, M. (2003). Multi-scale feature extraction on point-sampled surfaces, *Computer Graphics Forum*, Vol. 22, Blackwell Publishing, Inc, pp. 281–289.
- Pears, N. (2008). Rbf shape histograms and their application to 3d face processing, pp. 1–8.
- Pears, N. & Heseltine, T. (2006). Isoradius contours: New representations and techniques for 3D face registration and matching, *3DPVT'06: Proceedings of the Third International Symposium on 3D Data Processing, Visualization, and Transmission*, IEEE Computer Society, Washington, DC, USA, pp. 176–183.
- Perakis, P., Passalis, G., Theoharis, T., Toderici, G. & Kakadiaris, I. (2009). Partial matching of interpose 3d facial data for face recognition, *BTAS 2009: Proceedings of the IEEE Third International Conference on Biometrics: Theory, Applications and Systems*, Washington DC.
- Phillips, P., Grother, P., Micheals, R., Blackburn, D., Tabassi, E. & Bone, J. (2003). FRVT 2002: Evaluation report, *Technical Report NISTIR 6965*, NIST.
- Rusinkiewicz, S. & Levoy, M. (2001). Efficient variants of the ICP algorithm, *3DIM '01: Proceedings of the Third International Conference on 3D Digital Imaging and Modeling*, pp. 145–152.
- Russ, T., Boehnen, C. & Peters, T. (2006). 3D face recognition using 3D alignment for PCA, *CVPR '06: Proceedings of the 2006 IEEE Computer Society Conference on Computer Vision and Pattern Recognition*, IEEE Computer Society, Washington, DC, USA, pp. 1391–1398.
- Samir, C., Srivastava, A. & Daoudi, M. (2006). Three-dimensional face recognition using shapes of facial curves, *IEEE Transactions on Pattern Analysis and Machine Intelligence* **28**(11): 1858–1863.
- Sigg, C. (2006). *Representation and Rendering of Implicit Surfaces*, PhD thesis, ETH Zürich.
- Silverman, B. (1986). *Density estimation for statistics and data analysis*, Chapman & Hall/CRC.
- Smeets, D., Fabry, T., Hermans, J., Vandermeulen, D. & Suetens, P. (2009). Isometric deformation modeling using singular value decomposition for 3d expression-invariant face recognition, *Biometrics: Theory, Applications, and Systems, 2009. BTAS '09. IEEE 3rd International Conference on*, pp. 1–6.
- Sukumar, N. (2005). Maximum entropy approximation, *Bayesian Inference and Maximum Entropy Methods in Science and Engineering* **803**: 337–344.
- ter Haar, F. B. & Veltkamp, R. C. (2008). SHREC'08 entry: 3D face recognition using facial contour curves, *SMI '08: Proceedings of the IEEE International Conference on Shape Modeling and Applications*, Stony Brook, NY, USA, pp. 259–260.
- Tsin, Y. & Kanade, T. (2004). A correlation-based approach to robust point set registration, *ECCV (3)*, pp. 558–569.
- Vandermeulen, D., Claes, P., Loeckx, D., De Greef, S., Willems, G. & Suetens, P. (2006). Computerized craniofacial reconstruction using CT-derived implicit surface representations, *Forensic Science International* (159): S164–S174.
- Varshosaz, M., Helali, H. & Shojaee, D. (2005). The methods of triangulation, *Map Middle East '05: Proceedings of the 1st Annual Middle East Conference and Exhibition on Geospatial Information, Technology and Applications*, Dubai, UAE.

- Veleba, D. & Felkel, P. (2007). Survey of errors in surface representation and their detection and correction, *WSCG '07: Proceedings of the 15th International Conference in Central Europe on Computer Graphics, Visualization and Computer Vision*, Plzen-Bory, Czech Republic.
- Walder, C., Schölkopf, B. & Chapelle, O. (2006). Implicit surface modelling with a globally regularised basis of compact support, *Computer Graphics Forum* 25(3): 635–644.
- Wang, F., Vemuri, B., Rangarajan, A. & Eisenschenk, S. (2008). Simultaneous nonrigid registration of multiple point sets and atlas construction, *IEEE Transactions on Pattern Analysis and Machine Intelligence* 30(11): 2011–2022.
- Wang, Y., Pan, G., Wu, Z. & Wang, Y. (2006). Exploring facial expression effects in 3D face recognition using partial ICP, in P. Narayanan (ed.), *Computer Vision – ACCV 2006*, Vol. 3851 of *Lecture Notes in Computer Science*, Springer Berlin / Heidelberg, pp. 581–590.
- Yang, Y., Yong, J., Zhang, H., Paul, J. & Sun, J. (2006). Optimal parameterizations of bézier surfaces, pp. I: 672–681.
- Yano, K. & Harada, K. (2007). Single-patch nurbs face, *Signal-Image Technologies and Internet-Based System, International IEEE Conference on* 0: 826–831.